Available online at www.elixirpublishers.com (Elixir International Journal)

Vibrational Spectroscopy

Elixir Vib. Spec. 100 (2016) 43644-44648

ISSN: 2229-712X

Molecular structure and vibrational spectroscopic analysis of an anti HIV drug Epivir: A combined experimental and quantum chemical approach

Yugal Kishor Tiwari and R. A. Singh

Department of Physics Dr. Hari Singh Gour University Sagar 470001, India.

ARTICLE INFO

Article history:

Received: 4 October 2016;

Received in revised form:

9 November 2016;

Accepted: 17 November 2016;

Keywords

Anti HIV drug Epivir,

FT-IR Spectra,

FT Raman Spectra,

DFT calculations.

ABSTRACT

Epivir is an anti HIV agent belonging to the class of nucleosides reverse transcriptase inhibitors. These drugs interrupt the virus to make copy of it. A systematic quantum chemical study and vibrational spectra of Epivir has been reported. Structure and spectral characteristic of Epivir have been studied using vibrational spectroscopy and quantum chemical methods. Density function theory calculations of optimized geometry and vibrational spectra have been carried out by Gaussian03, using 6-311G basis set and B3PW91 functional. Based on these results we have discussed the correlation between these vibrational modes and crystalline structure of Epivir. A complete analysis of experimental IR and Raman spectra has been reported on the basis of wave number of the vibrational bands. The IR and the Raman spectra of the molecule based on DFT calculations shows reasonable agreement with the experimental results. The calculated HOMO, LUMO shows that the charge transfer takes place within the molecule.

1. Introduction

Acquired immunodeficiency syndrome (AIDS, is a disease in which body's immune system breaks down and is unable to fight off infection caused by human immune deficiency virus (HIV). HIV infects the human cells and uses the energy and nutrients provided by those cells to grow and reproduce. The highly active anti Retroviral (anti HIV)[1] therapy (HAART) has largely reduced the morbidity and the mortality of HIV infected patients, but a serious metabolic syndrome combining insulin resistance, dyslipidemia, central adiposity and peripheral lipoatropy has arisen in treated individuals. This highly active anti retroviral therapy includes protease inhibitors (PIs) and nucleoside reverse transcriptase inhibitors (NRTIs). The RT is a multifunctional enzyme that catalyses RNA dependent DNA polymerases, DNA dependent DNA polymerases. These all functions are required in the reproduction or replication of HIV, making RT central to the virus life cycle, the providing a primary target for anti HIV drugs which are widely used in the treatment of AIDS[2,3].

Epivir is widely using in the treatment of HIV positive and hepatitis B positive patients. Epivir is a synthetic nucleoside analog that is being increasingly used in the treatment of HIV infection [4, 5]. Epivir after oral administration rapidly get absorb, its bioavailability is 86% ± 16%, its peak serum concentration is 1.5 ± 0.5 mg/ml and mean elimination half life is 5 to 7 hours, and thus it is necessary to take it frequently so that the therapeutic drug level is maintained[6]. Epivir is a white to off-white crystalline solid with a solubility of approximately 70 mg per mL in water at 20°C. The solid state chemistry of this drug is of significant pharmaceutical interest as the drug is reported to exist in three crystalline forms. The two forms (Form I and II) reported in 1996 which were again studied by Harris et al in 1997.

Later in 2007, a new patent showing the existence of another polymorphic form III appeared. Michael et al have shown that Form I of Epivir has been prepared by dissolving Form II in hot water and then adding an equal volume of methanol to reduce the solubility of Epivir. The crystalline structure of Epivir have been reported by Ravi Kumar and Sridhar using X-ray diffraction, which revealed that the Form II was bipyramidal crystals with one molecule in the asymmetric unit and Form I showed five molecules in the asymmetric unit of crystal lattice. The form III is to be hemihydrates with two molecules of water associated with four molecules of Epivir in a crystal lattice [7].

Instead of the relevance of NRTIs in HAART therapy, vibrational spectroscopic investigations of these drugs are not fully explored. In present communication, spectroscopic analysis of Epivir molecule through quantum chemical calculation by density functional theory (DFT)[8] with Becke"s three parameter exchange function combined with Gradient Corrected correlation function of Perdew and Wang 1991 (B3PW91)[9-12] functional using 6-311G (d,p) basis set were carried out, which give the valuable information for the quality control of medicines. A complete vibrational analysis of Epivir is performed by combining Raman and IR data with quantum chemical calculations.

The method of vibrational spectroscopy specially have its importance in the characterization of supramolecular complexes because hydrogen bonding pattern and other "weak" interaction differ from one form to another and the functional group affected will display shifts in the each of the vibrational modes. The calculated vibrational spectra are analyzed and the different modes of vibration are explained, which allows interpretation of IR and Raman spectra.

Tele:

E-mail address: yugal.drhsgu@gmail.com

2. Computational Analysis

We mimic the crystalline structure by a small subset of a molecular unit shown in figure1. Complete information about the structural characteristics and vibrational mode of Epivir molecule is obtained by DFT using Gaussian 03[13, 14]. The vibrational spectrum is obtained at the same level of theory to test the stability of their computed molecular structure. A complete vibrational assignment is also conducted for Epivir, for this purpose the vibrational wave number in the harmonic approximation were calculated which also provide weightage value of internal co-ordinate for vibrational assignment.

In order to test the reliability of our modeling techniques we compare bond length and bond angle with the experimental values. Comparisons of experimental and theoretical values of bond length and bond angles are given in table 1 and table 2 respectively.

Since DFT vibrational number are known to be higher than experimental wave numbers due to neglect of anharmonicity effects they are scaled down by dual scaling procedure. Hall et al.[15] made a critical analysis of experimentally measured and theoretically calculated wave numbers at same level of theory and divided the normal modes in two regions. The region below 1800 cm^{-1} called finger print region and the region above 1800 cm^{-1} include X-H stretching mode [16]. Further as demonstrated in their report dual scaling give the better agreement between theoretical and experimental results. The dual scaling factor 0.9927 and 0.9659 for region below 1800 cm^{-1} and above 1800 cm^{-1} regions respectively are used in present study to avoid the systematic error caused by ignoring the anharmonicity and electron density [17,18]. The vibrational assignments of different modes were made by analyzing the result after calculations using Gauss view 4.1 program [19] finally calculated vibrational wave number gives the thermodynamic properties.

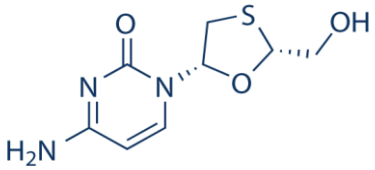

Fig 1.Ball stick model of the Epivir molecule.

Graphical representation of IR and Raman spectra were made by using Gauss view program by combining the results of the Gauss view program and with symmetry consideration vibrational wave number assignment were made with a high degree of accuracy. There are always some ambiguity in defining internal co-ordinates, however in this study the internal co-ordinates define form a complete set and the atomic motion of all the normal modes were observed using the Gauss view program.

3. Experimental details

Infrared spectra were recorded on a Shimadzu 8400 S-FT-IR spectrometer with a spectral resolution of 4 cm^{-1} in the region 400-4000 cm^{-1}. Sample was prepared from mixture of KBr in the ratio 99:1. The FT-Raman spectra were recorded on a RENISHAW INVIA Raman Microscope attach with He-Ne laser of wavelength 633nm in the region 400-4000 cm^{-1} using 10mw power. The sample was measured in a hemispherical bore of an aluminium sample holder.

4. Result and Discussion

4.1. Geometry optimization and energies

Since molecular geometry plays an important role in determining the structural activity relationship, the structural analysis provides meaningful information related to the drug action because in the case of flexible molecules, the receptor is likely to alter the solution conformation upon binding. Fig.2 shows the equilibrium state of Epivir. The molecular structure of Epivir belongs to the C1 point group symmetry, the structural parameter of the molecule obtained from geometry optimization are similar to the experimentally available data [20]. The comparison of theoretical and experimental bond length and bond angle is shown in Table.1 and Table.2 respectively.

Table 1. Theoretically calculated and experimentally observed bond length.

Bond Length	B3LYP	B3PW91	Experimental*
C1C4	1.5144	1.522	1.52
C1O25	1.447	1.407	1.40
C4S23	1.915	1.8620	1.84
C4O6	1.434	1.404	1.40
S23C21	1.874	1.812	1.80
C21C7	1.527	1.529	1.52
C7O6	1.455	1.415	1.40
C7N9	1.455	1.450	1.45
N9C19	1.435	1.436	1.40
C19O20	1.246	1.215	1.21
C19N18	1.369	1.359	1.33
C14N18	1.331	1.314	1.30
C14C12	1.433	1.432	1.40
C12C10	1.357	1.353	1.34
C10N9	1.368	1.356	1.33
C14N15	1.357	1.353	1.35

Table 2.Theoretically calculated and experimental bond angle.

Bond Angle	B3LYP	B3PW91	Experimental[20]
O25C1C4	112.31	112.61	110.56
C4C4O6	109.36	108.80	109.4
O6C4S23	107.50	108.09	107.8
C4O6C7	116.74	114.87	103.9
O6C7C21	109.30	108.02	109.4
C7C21S23	105.55	104.22	104.0
C21S23C4	89.31	90.63	90.2
O6C7N9	106.84	107.22	106.5
C21C7N9	112.19	112.55	110.8
C7N9C10	120.21	120.11	120.1
C7N9C19	118.00	117.96	116.4
N9C10C12	120.48	120.67	119.8
N9C19O20	118.73	118.44	121.7
N9C19N18	124.49	125.01	121.8
C19N18C14	121.05	120.88	119.8
C12C14N18	122.77	123.63	121.5
C12C14N15	120.41	119.41	116.1
N18C14N15	116.81	116.94	114.7

The equilibrium geometry has been determined by the energy minimization. The energy calculated by DFT B3PW91/ 6-311G is -1099.48598014 au and that by DFT/B3LYP/6311G is -1099.643 au.

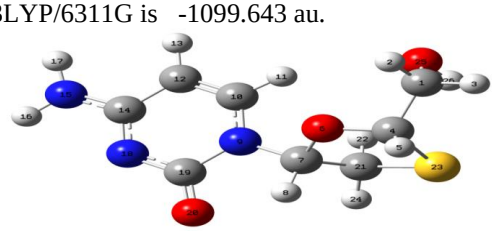

(a)

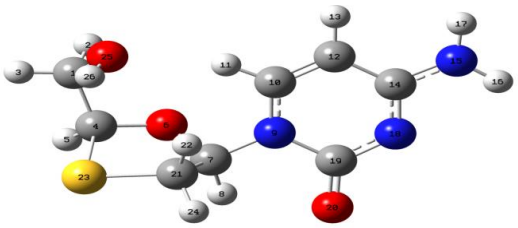

(b)

Fig 2. Optimized Geometry of Epivir Molecule (a) by DFT B3PW91/6-311G (b) by DFT B3LY/6-311G.

The conformational stability of Epivir is investigated by scanning the relative orientation of ring-1(the six membered ring) and ring-2 (five membered ring). The potential energy is determined by calculating the variation in the total energy of the molecule with change in dihedral angle (N18C14N15H17) by DFT/6-311G methods.

4.2.Vibrational analysis

The total number of atoms in Epivir molecule is 26 and it gives the total 72 (3N-6) normal modes. Experimentally obtained crystalline structure and the theoretically optimized structure shows that the molecule belongs to C1 point group symmetry hence all the 72 normal modes of vibration of the molecule are IR and Raman active. DFT calculation gives the Raman scattering amplitude which cannot be taken directly as the Raman intensity. The Raman scattering cross-section $\frac{\partial \sigma_j}{\partial \Omega}$, which are proportional to Raman intensity may be calculated from the Raman scattering amplitude and predicted wave number for each normal mode using the relationship [21,22].

$$\frac{\partial \sigma_j}{\partial \Omega} = \left(\frac{2^4\pi^4}{45}\right)\left(\frac{(v_0 - v_j)}{1 - exp\left[\frac{-hcv_j}{kT}\right]}\right)\left(\frac{h}{8\pi^2 cv_j}\right)S_j$$

Where S_j and υ_j are the scattering activities and the predicted wave numbers respectively of the jth normal mode, υ_0 is the wave number of the Raman excitation line and *h*, *c*, and *k* are universal constants.

The Raman intensities obtained from this relation give the excellent agreement with the experimentally observed values which are shown in Fig.3. The calculated IR Raman intensities were used to predict the vibrational mode with Lorentzian line shape (full width at half maximum= 8 cm^{-1}) to produce simulated spectra. The vibration assignments for the different mode have been made on the basis of relative intensities, energies and line shape. All vibrational bands have been assigned satisfactorily after proper analysis. All the assigned wave numbers of different modes were calculated which are shown in Table.3

4.3.Vibrational spectrum:

Comparison of wave number calculated by DFT / B3PW91 with experimental value reveals an over estimation of the wave number of vibrational mode due to neglect of anharmonicity in real system. Since the vibrational wave number obtained from the DFT calculations are higher than the experimental wave number, they were scaled down by wave number linear scaling procedure (WLS) [υ_{obs}/ υ_{cal}= (1.0087-0.0000163× υ_{cal})cm^{-1}] Yoshida et. Al.[23] and a comparison were made with the experimental values. The WLS method predicts the vibrational wave number with high accuracy and it is applicable to large number of molecule (compounds) except those where the effect of dispersion force is significant, the vibrational wave number calculated with approximate functions are often in good agreement with observed wave number when the calculated wave numbers are uniformly scaled with only one scaling factor. The calculated vibrational wave number in this study is the scaled value. Experimental and theoretical FT-IR and Raman spectra are shown in Fig.3 and Fig.4 from the figures it is clear that theoretical and experimental FT-IR and Raman frequencies are in excellent agreement with each other.

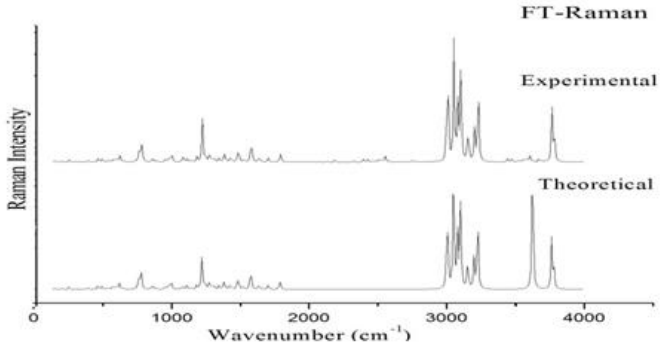

Fig 3. Theoretically calculated and experimental Raman scattering spectra in the region, 200- 4000 cm^{-1}.

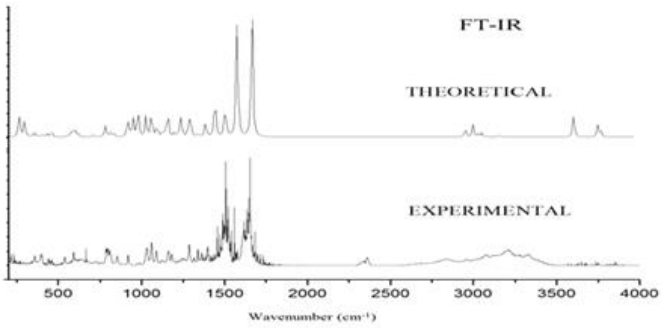

Fig 4. Theoretically calculated and experimental infrared absorbance spectra in the region, 200- 4000 cm^{-1}.

4.3.1 Ring-1/ six membered ring Vibrations:

The CH stretching vibrations give rise to multiple bands in the region 3000 cm^{-1} to 3100 cm^{-1}. The CH stretching in IR is found to be at 3207 cm^{-1} and 2961 cm^{-1}, and at 3220 cm^{-1}, 3195 cm^{-1}, 3113 cm^{-1}, 3020 cm^{-1} in Raman spectra where as its calculated value is 3115 cm^{-1},3110 cm^{-1}, 3000 cm^{-1} and 2945 cm^{-1}. The CH stretching vibrations are usually strong in both the IR and Raman spectra. The CC stretching is observed at 1768 cm^{-1},1680 cm^{-1} in Raman and 1770 cm^{-1}, 1653 cm^{-1} in IR where as it is calculated to be 1773 cm^{-1} and 1689 cm^{-1}.

The calculated value for NH_2 scissoring is 1622 cm^{-1} [24] it corresponds to the peaks at 1653 cm^{-1} in IR spectra and at 1654 cm^{-1} in Raman spectra. The NH_2 symmetric stretching is observed at 3650 cm^{-1} in Raman and at 3620 cm^{-1} in IR and its calculated value is 3622 cm^{-1}. The calculated value for CO wagging is 2912 cm^{-1} where as its corresponding peaks are found to be at 2910 cm^{-1} for Raman and 2908 cm^{-1} for IR spectra. The CH bending is observed at 1620 cm^{-1} in Raman spectra and 1621 cm^{-1} in IR spectra where as its calculated value is 1622 cm^{-1}. CN stretching is observes theoretically at 1513 cm^{-1} where as the corresponding peaks are found at 1513 cm^{-1} in Raman spectra.

CO wagging is observed at 1737 cm^{-1} in Raman and at 1732 cm^{-1} in IR and its calculated value is 1773 cm^{-1}. CN twisting is observed in Raman spectra at 1543 cm^{-1} where as its calculated value is found to be 1513 cm^{-1}. The calculated value of OH bending is 1412 cm^{-1} and this corresponds to the peak at 1410 cm^{-1} in IR spectra.

CO out of plane bending is observed at 789 cm^{-1} in Raman and at 786 cm^{-1} in IR spectra and its theoretically calculated value is 790 cm^{-1}. The ring deformation is calculated to be at 1427 cm^{-1} which corresponds to the peaks at 1430 cm^{-1} in IR spectra.CH out of plane bending is observed at 768 in IR spectra where as its calculated value is 772 cm^{-1}.

Table 3. Theoretical and experimental vibrational wave number (cm^{-1}) of Epivir.

Unscaled	scaled	IR	Raman	Assignment
3776	3647	3648	3662	R2 (OH stretching)
3759	3630	-	-	R1 (NH_2 asymmetric stretching),
3622	3498	3620	3650	R1 (NH_2 symmetric stretching),
3226	3115	-	3202	R1 (CH stretching)
3220	3110	3207	3195	R1 (CH stretching)
3154	3046	-	3042	R2 (CH_2 asymmetric stretching)
3105	3000	3184	3013	R2 (CH stretching) + C21H_2 symmetric stretching
3099	2993	3144	3056	R2 (C1H2 asymmetric stretching)
3078	2973	3074	3035	R2 (CH_2 Asymmetric stretching) + C7H8 stretching
3050	2945	2961	3020	R2 (CH stretching)
3015	2912	2908	2910	R2 (CH_2 symmetric stretching) + R2 (CH stretching)
1787	1773	1770	1768	R1 (C=C stretching)+ R1(C19O20 wagging)
1702	1689	1653	1780	R1 (NH_2 scissoring) + R1 (C=C stretching) + N15H_2 scissoring
1634	1622	1521	1620	R1 (NH_2 scissoring) + R1 deforming + C10H11 bending + C10H12 stretching
1575	1513	-	1543	R1 (C14N18 stretching) + C14N15 twisting + C10-C12 stretching + R1(CH bending)
1434	1427	1430	-	R2 (C7H8 wagging) + R2 (OH bending) + R1 deforming + C1H2 wagging
1423	1412	1399	1415	R2 (CH_2 scissoring) + R1 deforming + R2 (C1H_2 wagging) + OH bending
1392	1381	1362	-	R2 (C1H2 wagging) + R2 (C4H5 bending) + C1H_2 twisting
1341	1354	1286	1295	R1 (CH wagging) + R1 (NH2 wagging) + R2 (CH_2 wagging) + R2 (O-H bending) + R2 (CH bending)
1273	1263	1178	1260	R2 (C21H2 wagging) + R1 (NH bending) + R1 deforming
1212	1203	1183	-	R1 (N-H stretching)+ R1 (C1H_2 twisting) + R2 (OH bending)+ R2 (OH stretching)
1136	1127	1119	-	R2 (C1H2 twisting) + O25H2 bending + R2 deforming
1082	1074	1033	1056	R1 (C19-H15stretching) + R1 (OH bending) + NH rocking + R2 deforming
961	953	-	980	R2 (N15H2 rocking) + R1 deforming
948	941	945	-	R2 (C21H2 rocking) + R1 (CH bending)
882	875	890	-	R2 (C1H2 rocking) + R2 deforming + NH bending
856	849	843	-	R2 (N9C7 stretching) + R2 deforming + R2 (CH rocking)
796	790	786	789	R1 (CO out of plane bending) + R1deforming + R2 (SC stretching)
778	772	768	-	R1 (CH out of plane bending) + R1 (C12H13 wagging)
764	758	668	-	R2 (S23H21 stretching) + R2 deforming + R1 deforming + CH stretching
756	750	-	723	R1(NC stretching) + R2 deforming + R2 (SC4 bending)
729	723	635	721	R1 (C12H13 wagging) + R2 (CO bending)
645	640	595	637	R1 C19 out of plane bending
617	612	-	612	R1 and R2 deforming + R1 (NH2 rocking) + OH bending
595	590	541	584	R1 and R2 deforming + OH wagging
528	524	-	516	R1 and R2 deforming + R2 (CH rocking) + R1(NH2 twisting) + R2 (OH bending)
387	384	-	-	R1 deforming + R2 deforming + R1 (CH out of plane bending) + NH twisting + R1 (C1H2 rocking)
370	367	-	365	R1 (NH2 rocking) + CO bending + CH2 twisting
250	248	-	252	R2 (C1H_2 twisting) + R2 deformation + C9N7 bending + R1 bending
210	208	-	-	R1 (N15H_2 wagging) + R2 (CH2 rocking) + R2 bending
147	146	-	-	R1 (NH2 wagging) + R1deforming + R2 (CH2 rocking)
98	97	-	-	R1 (NH wagging) + R2 (OH bending)
55	54	-	-	R2 (CH2 bending) + OH out of plane bending

4.3.2. Ring-2/ five menbered ring Vibrations

The OH stretching experimentally is observed at 3662 in Raman spectra and at 3648 cm^{-1} in IR spectra where as its calculated value is found to be 3647 cm^{-1}[25] CH_2 symmetric stretching is found to be at 3013 cm^{-1} in Raman spectra where as its calculated value is 3000 cm^{-1}. CH stretching is found at 2908 cm^{-1}, 2961 cm^{-1} in IR and at 2910 cm^{-1} and 2940 cm^{-1} in Raman spectra and its calculated value is 2912 cm^{-1} and 2945 cm^{-1}. The calculated value for CH wagging is 1427 cm^{-1}, 1412 cm^{-1} and it is observed at 1430 cm^{-1}, 1399 cm^{-1} in IR spectra and at 1415 cm^{-1} in Raman spectra. CH bending is found at 1362 cm^{-1} in IR spectra where as its calculated value is 1381 cm^{-1}. OH bending in theoretical calculation is found at 1427 cm^{-1},1354 cm^{-1} and the corresponding peaks is found at 1430 cm^{-1}, 1286 cm^{-1} in IR spectra and at 1295 cm^{-1} in Raman spectra. OH stretching is found at 1183 cm^{-1} in IR spectra and corresponding theoretical value is found to be 1203 cm^{-1} an other peak for OH stretching is found in Raman spectra is found at 612 cm^{-1} and its theoretical value is also found 612 cm^{-1}.

The NH rocking is observed at 980 cm^{-1} in Raman spectra and its theoretically calculated value is found to be 953 cm^{-1}. The peaks corresponding to CH rocking is found at 945 cm^{-1} in IR spectra and its calculatd value is 941 cm^{-1}. CN stretching is found at 843 cm^{-1} in IR spectra and calculated value is found to be 849 cm^{-1}. The deformation in ring is observed at 1033 cm^{-1}, 890 cm^{-1}, 541 cm^{-1} in IR spectra and at 1056 cm^{-1}, 584 cm^{-1} in Raman spectra where as its calculated value is 1074 cm^{-1}, 875, 590 cm^{-1}. SC stretching is found theoretically at 790 where as it is observed at 786 cm^{-1} in IR spectra and at 789 cm^{-1} in Raman spectra. SH stretching is observed in IR

spectra at 768 cm^{-1} and where as its calculated value is 750 cm^{-1}. CO bending is calculated to be 723 cm^{-1} and corresponding peaks are found at 721 cm^{-1} in Raman spectra and at 635 cm^{-1} in IR spectra. The OH wagging is found at 541 cm^{-1} in IR spectra and at 584 cm^{-1} in Raman spectra where as its calculated value is found to be 590 cm^{-1}. It is clear from the above observations that most of the theoretical and experimental values are in good agreement with each other.

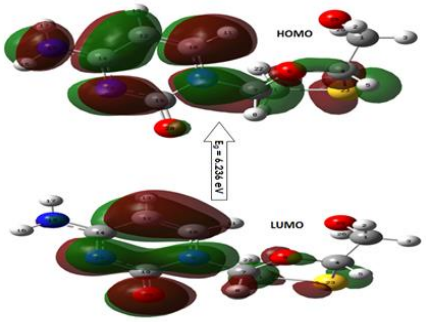

Fig 5. HOMO and LUMO of the Epivir molecule.

Table 4. The calculated thermodynamic and Electronic parameters of Epivir.

	Parameter	B3LYP	B3PW91
Thermodynamic	Total energy (au)	-1099.6423	-1099.485
	Zero point energy (kcal/mol)	126.46	124.24
	Vibrational Entropy	45.44	44.23
Electronic	Dipole Moment (Debye)	5.96	4.791
	HOMO (eV)	-6.040	-7.18
	LUMO (eV	-0.945	-0950
	Energy Gap (eV	5.095	6.236

4.4. Thermodynamic and electronic properties

The thermodynamic parameters of Epivir have also been computed by DFT B3PW91 and DFT B3LYP methods and are presented in Table 4.

The total energies, vibrational motion contribution to entropy, rotational constants, Highest Occupied Molecular Orbital (HOMO) and Lowest Unoccupied Molecular Orbital energy (LUMO), energy gap between HOMO and LUMO and dipole moment values are obtained from DFT/B3PW91 and DFT/ B3LYP methods. The energies of Epivir by DFT B3PW91 and B3LYP methods are -1099.485 and -1099.6423 au. respectively. The variation in the Zero point Vibrational energies seems to be insignificant.

5. Conclusion

Vibrational spectroscopy and density functional theory calculation has been applied to the structural and spectroscopic investigation of Epivir. The equilibrium geometry and vibrational wave numbers for all the 72 mode of the molecule were determined and analyzed with DFT/B3PW91 applying 6-311G basis set, giving allowance for the lone pair through the diffused functions. The comparison between theoretically and experimentally observed wave number from IR and Raman spectra reveals that the experimental and theoretical results are in good agreement. A detailed normal coordinate analysis of all the normal modes clearly illustrates the composition of each normal mode in terms of internal coordinate. In present study the complete vibrational assignment along with all structural and thermo dynamical parameters of Epivir is presented and we believe that the results obtained herein will prove to be an excellent starting point for studying the detailed potential surface of the molecule which is needed to understand the drug receptor interactions. Dissimilarities if any, between observed and calculated wave numbers is due to the fact that the calculations have been performed on single molecule in gaseous state. Thus reasonable deviation from the experimental values seems to be justified.

References

1. E. De Clercq, AIDS Res. Hum. Retroviruses 8 (1992) 119–134.
2. J. Ren, R.M. Esnouf, A.L. Hopkins, J. Warren, J. Balzarini, D.I. Stuart, D.K. Stammers, Biochemistry 37 (1998) 14394–14403.
3. S. Mishra, P. Tandon, A.P. Ayala, Spectrochimica Acta Part A 88[2012] 116-123
4. Katlama C, ValantinMA, Matheron S, CoutellierA,Calvez V, D Descamps D, Longuet C, Bonmarchand M, Tubiana R, De Sa M, Lancar R,Agut H, Brun-Vezinet F, and Costagliola D. Efficacy and tolerability of stavudine plusEpivir in treatment-naive and treatment experienced patients with HIV- infection. AnnIntern Med. 1998;129:525-531.
5. Merrill DP, Moonis M, Chou TC, Hirsch MS. Epivir or stavudine in two- and three-drug combinations against human immunodeficiency virus type 1replication in vitro. J Infect Dis. 1996; 173:355-364.
6. Himadrisen, Surva Kumar J, inventors. Long acting composition containing zidovudine and Epivir. US patent publication US20050175694A1. August 11, 2005. [4] C. K. Chu, J. W. Beach, L.S. Jeong, B. G. Choi, F. Comer, A.J. Alves and R. F. Schinazi, J. Org. Chem. 1991,56,6503
7. K. Ravikumar, B. Sridhar, Mol. Cryst. Liq. Cryst. 515 (2009)
8. P. Kohenberg, W. Kohn, Phys. Review. B 864 [1964] 136.
9. A.D. Becke, Phys. Rev. A 38 (1988) 3098–3100.
10. C.T. Lee, W. Yang, R.G. Parr, Phys. Rev. B 37 (1988) 785.
11. R.G. Parr, W. Yang, Density Functional Theory of Atoms and Molecules, Oxford University Press, New York. (1989).
12. A.D. Becke, J Chem. Phys., 89 (1993) 5648.
13. M.J. Frisch, et al., Computer Program Gaussian 03W, Gaussian Inc., Pittsburgh, PA, USA, 2003.
14. A. Srivastava, S. Mishra, P. Tandon, S. Patel, A.P. Ayala, A.K. Bansal, H.W. Siesler, J. Molecular Structure, 964, (2010) 88-96.
15. M.D. Halls, J. Velkovski, H.B. Schlegel, Theor. Chem. Acc. 105 (2001) 413–421.
16. R.M. Silverstein, G.C. Bassler, T.C. Morrill, Spectrometric Identification of Organic Compounds, 5th ed., John Wiley & Sons, Inc., New York, 1981
17. S. Mishra, D. Chaturvedi, P. Tandon, V.P. Gupta, A.P. Ayala, S.B. Honorato, H.W. Siesler, J. Phys. Chem. A 113 (2009) 273–281.
18. J.M.L. Martin, C. Van Alsenoy, Computer Program GAR2PED, University of Antwerp, 1995.
19. A. Frisch, A.B. Nielson, A.J. Holder, GAUSSVIEW User Manual, Gaussian Inc., Pittsburgh, PA, USA, 2000.
20. Carl Kemnitz 2002 Chemoffice ultra 10, Trial version.
21. P. L. Polavarapu, J. Phys. Chem. 94 (1990) 8106.
22. G.A. Guirgis, P. Klaboe, S. Shen, D.L. Powell, A. Gruodis, V. Aleka, C.J. Nielsen, J. Tao, C. Zheng, J.R. Durig, J. Raman Spectroscopy, 34 (2003) 322.
23. H. Yoshida, K. Takeda, j. Okamura, A. Ehara, H. Matsurra, J. Phys. Chem. A. 106 (2002) 3580-3586.
24. Socrates G, Infrared and Raman Characteristic Group Frequencies – Tables and Charts, John Wiley and Sons, (2004)
25. G.A. Guirgis, P. Klaboe, S. Shen, D.L. Powell, A. Gruodis, V. Aleka, C.J. Nielsen, J. Tao, C. Zheng, J.R. Durig, J. Raman Spectroscopy, 34 (4) (2003) 322-33.